Ornamental Plant Research

ARTICLE

Open Access

https://doi.org/10.48130/OPR-2023-0021

Ornamental Plant Research **2023**, 3:21

Morphological, physiological and transcriptomic analyses reveal potential candidate genes responsible for salt stress in *Rosa rugosa*

Shuai Qi[1#], Xiaobin Wang[1#], Qikui Wu[1], Shutang Xing[2], Xuejian Li[1], Fei Zhao[2*] and Yunyan Yu[1*]

[1] *Shandong Provincial Research Center of Demonstration Engineering Technology for Urban and Rural Landscape, College of Forestry, Shandong Agricultural University, Tai'an 271018, China*

[2] *College of Horticulture Science and Engineering, Shandong Agricultural University, Tai'an 271018, China*

[#] These authors contributed equally: Shuai Qi, Xiaobin Wang

[*] Corresponding authors, E-mail: fly@sdau.edu.cn; yxyxst@sdau.edu.cn

Abstract

Rosa rugosa is a multifunctional species with various applications in fragrance extraction and ornamental, medical, and edible purposes. Compared to other species of *Rosa*, *R. rugosa* exhibits greater resistance to salt stresses; however, the mechanisms underlying its salinity tolerance are still unclear. Thus, we assessed the salt tolerance of 16 *R. rugosa* germplasms based on the changes in morphology and physiology under different salt concentrations. Among them, two cultivars ('Zizhi' and 'Fenzizhi') were chosen for transcriptome sequencing. The differentially expressed genes (DEGs) associated with phytohormone synthesis and signalling pathways, ROS production, carbohydrate metabolism and transport, stress response and resistance were identified as responding to salt stress in *R. rugosa*. PPI network analysis further identified two DEGs, *SCL28* and *E2F1*, which exhibited the most interactions with other DEGs. Consequently, this research contributes to a greater understanding of salinity tolerance mechanism in *R. rugosa* and could provide gene resources for breeding salt-tolerant cultivars in *Rosa*.

Citation: Qi S, Wang X, Wu Q, Xing S, Li X, et al. 2023. Morphological, physiological and transcriptomic analyses reveal potential candidate genes responsible for salt stress in *Rosa rugosa*. *Ornamental Plant Research* 3:21 https://doi.org/10.48130/OPR-2023-0021

Introduction

The natural environment exposes plants to diverse abiotic stresses, including extreme temperatures, waterlogging, and high salt concentrations, with soil salinization being the worst[1]. Soil salinization worsens due to environmental degradation, climate change, poor irrigation practices, poorly regulated fertilizer use, and industrial pollution[2,3]. Salinization affects approximately 20% of irrigated land and is projected to grow about 50% by the mid-21st century[4,5]. Salt stress severely limits plant growth, quality, and yield. Two primary strategies for mitigating soil salinity include restoring damaged soil or breeding and cultivating salt-tolerant cultivars, the latter being more secure and effective[6,7].

Rosa rugosa, a diploid species belonging to the Rosaceae family that is indigenous to East Asia, has high economic value due to its multifunctional properties. *R. rugosa* has the potential to be utilized for various purposes, such as fragrance extraction and ornamental, medical, and edible purposes. The essential oil extracted from *R. rugosa* is the most precious plant essential oil in the world, known as 'liquid gold'. *R. rugosa* displays superior resistance to both biotic and abiotic factors when compared to other species of *Rosa*. Some wild *R. rugosa* are distributed in coastal sandy or gravel soils and a few specific cultivars have been widely cultivated as ornamental plants in coastal cities with soils with high salt content, which indicates that there are types of cultivars with strong salt tolerance. Due to its remarkable adaptability, *R. rugosa* is an invasive species in northern Europe.

Salinity affects the physiological, morphological and molecular processes of plants, which eventually disrupts normal growth and metabolism[8]. The process of salt stress is characterized by two stages: osmotic stress in the early phase and ionic toxicity in the later phase[9]. Prolonged saline conditions lead to an increase in active oxygen, such as mono-oxygen, superoxides, hydroxyl radicals, and hydrogen peroxide[10]. Excessive ROS damage the plant cell membranes and DNA and affect vital biological activities, such as protein synthesis and photosynthetic pigment reduction[11]. Subsequently, plants transmit specific stress signals and adopt several adaptive strategies to adapt to saline environments. The plant response to salt stress involves multiple processes, such as ion transport, osmotic adjustment, phytohormone regulation, antioxidant regulation, and salt stress-responsive gene regulation[12].

In this study, we assessed the salt tolerance of 16 *R. rugosa* germplasms by examining their morphological and physiological characteristics under varying levels of salinity. Then, two cultivars, i.e., 'Zizhi' and 'Fenzizhi', were selected for further study due to their significant contrast in salt resistance and similarity in terms of morphology. To investigate the mechanisms underlying salt tolerance, we performed RNA-sequencing of roots in the 'Zizhi' and 'Fenzizhi' cultivars and analysed the DEGs related to salt stress. The aim of this study was to deepen our knowledge of the mechanisms underlying salt tolerance in *R. rugosa*.

Materials and methods

Plant materials and treatments

Two-year-old *R. rugosa* cutting seedlings were collected from the Rosaceae Germplasm Nursery located in the Forestry

Experimental Station of Shandong Agricultural University, Tai'an, China (36°10'15" N, 117°09'25" E)'. A total of 16 different germplasm-cutting seedlings were planted in a plastic container with a diameter of 260 mm and 3.4 kg of garden soil.

Containers with holes at the bottom and trays were used and placed in the Shandong Agricultural University Horticultural Greenhouse in March. After three months of growth, 1,152 seedlings from 16 germplasms ('Zizhi': ZZ; 'Fenzhongguan': FZG; 'Ciguo': CG; 'Zhongke-2': ZK-2; 'Hunchun': HC; 'Tangfen': TF; 'Tangzi': TZ; 'Xizi': XZ; 'Henan-2': HN-2; 'Baizizhi': BZZ; 'Fenzizhi': FZZ; 'Saixizi': SXZ; 'Zhulongyoukong': ZLYK; 'Henan-1': HN-1; 'Tanghong': TH; 'Zhuzishuanghui': ZZSH) were selected for further experiments. Salinity stress was induced in the 16 germplasms using NaCl solutions with varying concentrations (0.3%, 0.5%, and 0.7%). The control groups were irrigated with water only, but the stress groups were irrigated with salinated water of corresponding salt concentrations. The solution was divided equally and watered over three days to avoid a salt shock reaction. Following the achievement of the final concentration, the treatment period was recorded.

Salt injury indices

The morphology of plants was observed at 0, 4, 7, 10, and 16 d after stress (DAS) of 0.3%, 0.5%, and 0.7% salt treatment. The salt tolerance of *R. rugosa* was classified into six salt injury indices (SIIs): 0 (no injury); 1 (10% of the leaves are yellow); 2 (30% of the leaves are yellow, and leaves wilting or curling slightly); 3 (50% of leaves are yellow, and leaves wilting or curling even with a few leaves falling off); 4 (80% of leaves are scorched, large numbers of leaves fall off); and 5 (the plant is dead).

Growth and physiological indices

Net growth of new branch length ($\Delta L = L_{10} - L_0$), leaf relative water content (LRWC), and plant biomass were measured at 10 DAS in the 0, 0.3%, and 0.5% NaCl treatments. ΔL ($L_{10} - L_0$) is the growth of branch length at 10 DAS.

The third and fourth leaves from the top in the control groups and the 0.3% and 0.5% NaCl-treated groups were collected at 10 DAS for physiological measurements. Each sample had three replicates. The measurement of relative conductivity (REC) was carried out[13]. The leaching method was used to measure the chlorophyll (Chl) content[14]. The anthrone method was utilized to determine soluble sugar (SS) content[15]. The Coomassie brilliant blue technique was employed to ascertain the reference soluble protein (SP) level. Malondialdehyde (MDA) was calculated using the TBA technique[16]. Nitroblue tetrazolium photoreduction was used to evaluate superoxide dismutase (SOD) activity[17]. The guaiacol technique was used to determine peroxidase (POD) activity[17].

Transcriptome library construction and Illumina sequencing

Two cultivars, salinity-tolerant 'Zizhi'(ZZ) and salinity-sensitive 'Fenzizhi'(FZZ), were selected for transcriptome analysis. Twelve samples of roots from the control and 0.5% NaCl-treated groups at 4 DAS were collected for extracting total RNA with the Plant Total RNA Isolation Kit (Vazyme, Nanjing, China). The quality, purity, and integrity of the RNA were then assessed. cDNA libraries were prepared, normalized, and sequenced using a NovASeq 4000 (Illumina, CA, USA). The library comprised four samples (in triplicate): Z-CK (roots control in ZZ), Z-NaCl (4d salinity stress of roots in ZZ), F-CK (roots control in FZZ), and F-NaCl (4d salinity stress of roots in FZZ).

Screening and functional analysis of DEGs

The acquired clean reads were aligned using HISAT2 v2.1.0 to the *R. rugosa* genome database (http://eplantftp.njau.edu.cn/Rosa_rugosa/) to comprehend their functionalities. StringTie 1.1.3b was used to accomplish new transcript prediction. The gene expression level was assessed by quantifying the reads using the fragments per kilobase of exon model per million mapped fragments (FPKM) methodology. The differentially expressed (DEGs) were identified by setting the log2|fold changes| ≥ 2 and p-value ≤ 0.05 as criteria allowed for the examination of differential expression between samples. Gene Ontology (GO) annotation and Kyoto Encyclopedia of Genes and Genomes (KEGG) enrichment analyses were performed to gain further insights into the functions of DEGs. Finally, we generated a protein-protein interaction (PPI) network graph by using the STRING database (https://cn.string-db.org/cgi/input?sessionId=bnwcGhIHpZEW&input_page_show_search=on) combined with Cytoscape software.

qRT-PCR verification

The primers of 12 DEGs were designed and are listed in Supplemental Table S1. The qRT-PCR experiments were performed using the SYBR Green qPCR kit (Accurate Biology, China), and a CFX96 Real-time System was used for all procedures. *RrGADPH* served as an internal control during the $2^{-\Delta\Delta CT}$ analysis of the expression patterns. Each sample was biologically replicated three times.

Results

Morphological changes in response to salt stress

We evaluated the salt tolerance of 16 *R. rugosa* germplasms by observing the morphological changes under varying salt concentrations (0.3%, 0.5%, and 0.7%) and determined the salt injury index (SII: 0–6). The yellowing of leaves with increasing salt concentration was accompanied by significantly different salt tolerances among germplasms. Under 0.3% NaCl treatment, 'ZZ' and 'FZG' appeared with symptoms (SII1) at 10 DAS and reached SII2 at 16 DAS; conversely, the other 14 germplasms reached SII1 at 4 DAS. Among these 14 germplasms, eight germplasms and six germplasms reached SII3 and SII4, respectively, at 16 DAS. When exposed to 0.5% NaCl, all the germplasms exhibited symptoms (SII1–4) at 4 DAS. Eventually, 10 germplasms reached SII4, of which two cultivars, 'ZZ' and 'FZG' showed symptoms (SII2) at 10 DAS, 3 d later than the other eight germplasms. Of the remaining six germplasms, three germplasms, 'ZZSH', 'ZLYK', and 'HN-1' reached SII5 at 7 DAS and were more sensitive to salt treatment. Similar to the 0.5% NaCl treatment, all *R. rugosa* germplasms exhibited yellow leaves (SII1–4) at 4 DAS under the 0.7% NaCl treatment. 'ZZ' and 'FZG' reached SII4 at 16 DAS, whereas the other germplasms achieved SII5 at either 7 DAS or 16 DAS (Supplemental Table S2). Through cluster analysis of SII, 16 *R. rugosa* germplasms were categorized into two distinct groups based on salt tolerance. The salt-tolerant group consisted of 10 germplasms that could be further divided into two subgroups. 'ZZ' and 'FZG' showed greater salt resistance than the remaining eight germplasms. The salt-sensitive group was composed of six germplasms, of which 'ZLYK', 'HN-1', 'TH', and 'ZZSH' were more sensitive (Fig. 1a).

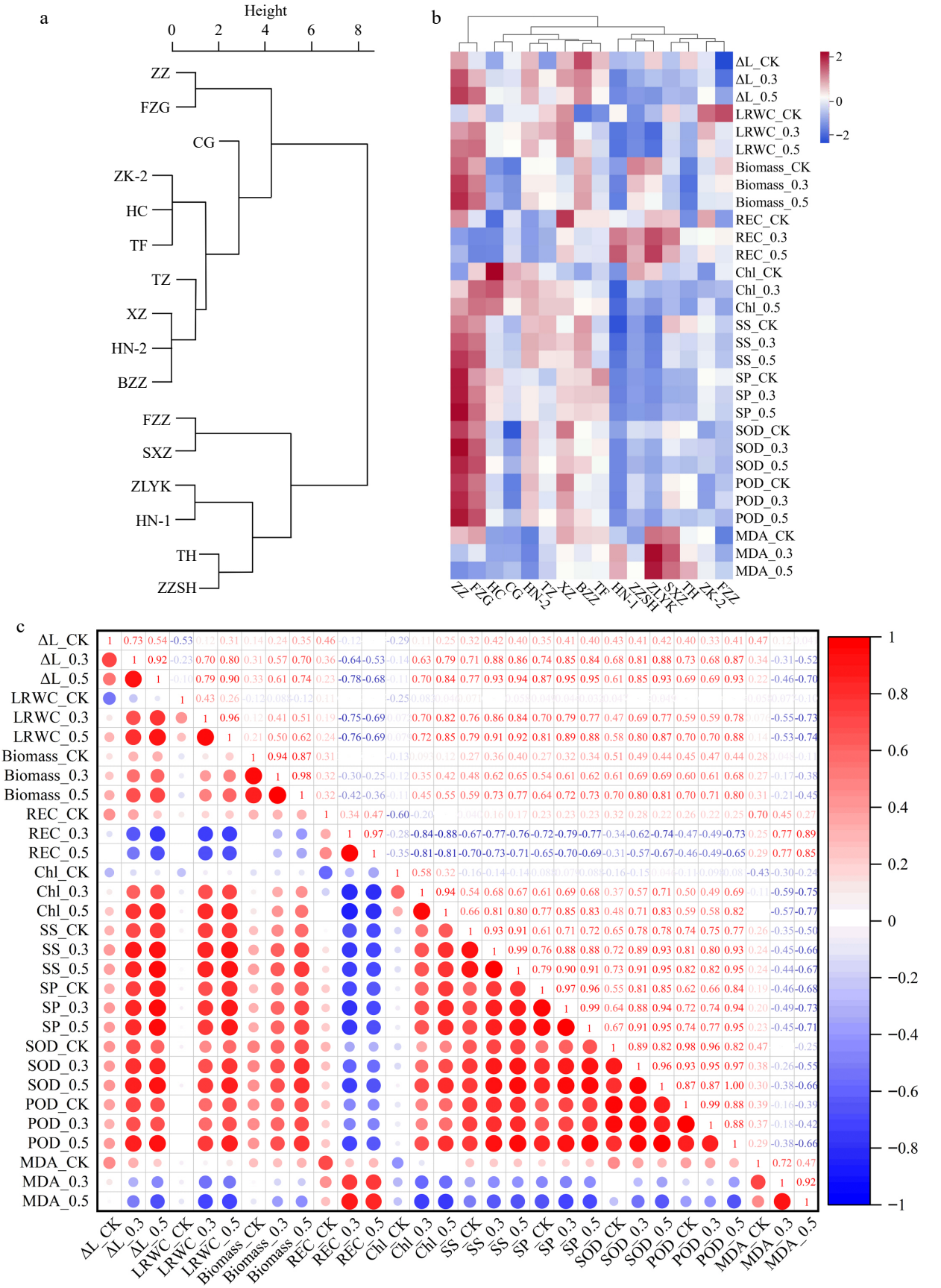

Fig. 1 Analysis of salt tolerance of 16 *R. rugosa* germplasms. (a) Cluster analysis of salt tolerance in *R. rugosa* according to salt injury index. (b) Clustering heatmap of growth and physiological indicators. (c) Correlation analysis of growth and physiological indicators.

Growth and physiological responses to salt stress

To make a more comprehensive evaluation of salt tolerance in 16 *R. rugosa* germplasms, three growth indicators and seven physiological indicators were measured at 10 DAS under 0%, 0.3%, and 0.5% NaCl treatments. As the NaCl concentration increased, a significant decrease in the three growth indicators (ΔL, LRWC, and plant biomass) and a significant increase in the physiological indicators (REC, SS, SP, MDA, SOD, and POD) were observed, except for Chl content, which displayed a decreasing trend (Supplemental Table S3).

Heatmap clustering was performed using ten indicators to evaluate the salt tolerance of sixteen germplasms (Fig. 1b). These germplasms were categorized into three distinct clusters, namely the salt-tolerant type ('ZZ' and 'FZG'), middle salt-tolerant type including seven germplasms ('HC', 'CG', 'HN-2', 'TZ', 'XZ', 'BZZ' and 'TF'), and salt-sensitive type including seven cultivars ('NH-1', 'ZZSH', 'ZLYK', 'SXZ', 'TH', 'ZK-2' and 'FZZ'). This finding is analogous to the clustering results of Fig. 1a. The strong salt tolerance of the *R. rugosa* germplasms showed that ⊿L, LRWC, plant biomass, Chl content, REC, and MDA underwent small fluctuations, while SS, SP, SOD, and POD showed significant changes compared to the control group. The 'ZZ' and 'FZG' cultivars exhibited the strongest salt tolerance. These observations clearly demonstrate that the salt tolerance of *R. rugosa* germplasms varies significantly.

The findings depicted in Fig. 1a & b were consistent with the results of principal component analysis (PCA). The explained variances of PC1 and PC2 are 52.31% and 13.04%, respectively (Supplemental Fig. S1). To determine the practical physiological parameters that could pinpoint *R. rugosa* salt tolerance, a correlation study was carried out. All of the indicators of treatment with 0.3% and 0.5% NaCl showed a high positive connection, with Pearson correlation coefficients ranging from 0.88 to 0.99 (Fig. 1c). Hence, measuring only one concentration of the indicator in further studies would suffice. Additionally, REC and MDA exhibited inverse correlations with the rest of the indicators, whereas other indices were positively correlated among themselves.

Identification of differentially expressed genes by transcriptome sequencing

Transcriptome sequencing was carried out to investigate the mechanical response to salinity stress using root samples of two cultivars (salinity-tolerant 'ZZ' and salinity-sensitive 'FZZ') at 0 and 4 DAS after 0.5% NaCl treatment. The raw data are available at the NCBI Sequence Read Archive with the accession numbers SRR25020864~SRR25020875. Twelve RNA libraries were generated from the RNA sequencing data, with Q20 and Q30 values greater than 98.11% and 94.31%, respectively. The average GC content was approximately 45.14% (Supplemental Table S4). Four comparison groups were constructed, namely, Z-NaCl vs Z-CK, F-NaCl vs F-CK, F-CK vs Z-CK, and F-NaCl vs Z-NaCl, resulting in 7,806 DEGs found in at least one group. Among these groups, 795, 2,207, 4,673, and 4,914 DEGs were identified, respectively, and among them, most genes were downregulated (Fig. 2a). There were 340 genes identified to exhibit differential expression in both cultivars, while 3,129 DEGs were discovered in the comparison of different cultivars. Moreover, only 43 genes had different expression patterns in all four groups (Fig. 2b).

GO and KEGG enrichment analysis

The DEGs of the Z-NaCl vs Z-CK group were categorized according to the GO database into biological processes (BP, 434), molecular functions (MF, 291), and cellular components (CC, 107) (Supplemental Table S5). On the other hand, the DEGs of F-NaCl vs F-CK were also categorized according to the GO database into BP (477), MF (302), and CC (117) (Supplemental Table S6). To further investigate the significance relevance of the salt stress-responsive DEGs, we analysed the top 10 terms that were enriched among the three groups (Fig. 2c & d). DEGs in ZZ and FZZ were mapped into 106 and 104 KEGG pathways, respectively (Supplemental Tables S7 & S8). Only two metabolic pathways (Ribosome, Ko03010, 81 genes; Oxidative phosphorylation, Ko00190, 34 genes) were significantly enriched (p-value < 0.05). There was no significantly enriched pathway in FZZ, while ribosome (Ko03010, 56 genes), carbon metabolism (Ko01200, 56 genes), and plant hormone signal transduction (Ko04075, 52) had the largest number of genes (Fig. 2e & f).

DEGs implicated in the biosynthesis, transport, and signalling of phytohormones

Genes involved in phytohormone biosynthesis and signal transduction showed different expression levels under salt stress in the two cultivars (Fig. 3). Notably, there were significant downregulation trends of 26 positive regulatory DEGs associated with auxin biosynthesis, transport and signal transduction in one or both cultivars, including *YUC* (evm.model.Chr6.539; evm.model.Chr2.1946), *PIN* (evm.model.Chr7.3286; evm.model.Chr7.3273; evm.model.Chr7.3546; evm.model.Chr6.1170), genes coding auxin transporter-like protein (evm.model.Chr2.6044) and auxin-induced protein (evm.model.Chr2.5904; evm.model.Chr4.2260), auxin efflux carrier component (evm.model.Chr1.4080; evm.model.Chr4.72; evm.model.Chr6.6477; evm.model.Chr6.4089), *IAA14* (evm.model.Chr1.692), *ARF* (evm.model.Chr5.2402), *GH3.17* (evm.model.Chr1.2987), *ARG7* (evm.model.Chr6.4936), and eight *SAUR* (evm.model. Chr6.4937; evm.model.Chr2.4303; evm.model.Chr2.4302; evm.model.Chr2.920; evm.model.Chr4.2643; evm.model.Chr2.664; evm.model.Chr5.5043; evm.model. Chr7.1017). Furthermore, one auxin-repressed gene, *ARP* (evm.model. Chr5.6322) was upregulated under NaCl treatment in both cultivars.

Eleven genes coding gibberellin-regulated proteins were identified as DEGs, including *GA20ox* (evm.model.Chr3.2679), *GA2ox* (evm.model.Chr5.6683; evm.model.Chr1.4538), *RGL1* (evm.model.Chr7.1135), *SCL* (evm.model.Chr5.1439; evm.model.Chr7.1860; evm.model.Chr6.5835), and *GRP* (evm.model.Chr2.893; evm.model.Chr6.1385; evm.model.Chr7.406; evm.model.Chr6.6415). Similar to DEGs involved in auxin, the expression patterns of gibberellin-related DEGs were downregulated under salt stress, except for one member of *GRP1* (evm.model.Chr2.893), which was upregulated after salt treatment.

Twelve genes were identified as DEGs in the abscisic acid regulation pathway. Specifically, the study found that *ABAH4* (evm.model.Chr2.5211) and *PYL4* (evm.model.Chr3.4190) exhibited downregulation. Moreover, nine members of *PP2C* (evm.model.Chr5.1398; evm.model.Chr6.681; evm.model.Chr7.1472; evm.model.Chr3.4893; evm.model.Chr5.1350; evm.model.Chr5.1020; evm.model.Chr2.6117; evm.model.Chr2.5507; evm.model.Chr6.898) and one *SnRK* (evm.model.Chr6.3894) gene were upregulated under salt stress, whereas only one member of *PP2C* (evm.model.Chr2.6117) was downregulated.

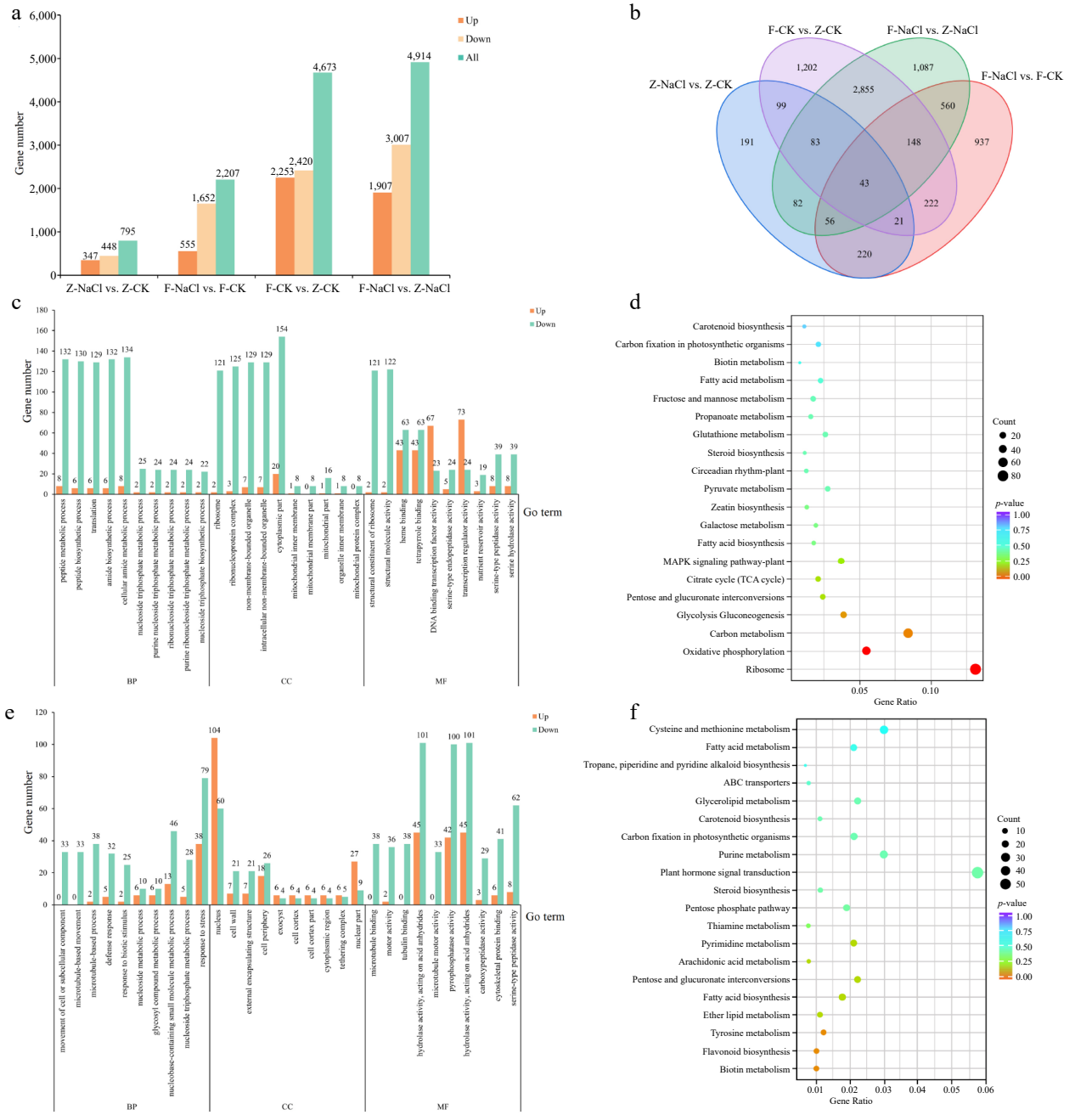

Fig. 2 DEG analysis of in the four comparison groups. (a) Total number of DEGs in Groups Z-NaCl vs Z-CK, F-NaCl vs F-CK, F-CK vs Z-CK, and F-NaCl vs Z-NaCl. (b) Venn diagram of DEGs in Z-NaCl vs Z-CK, F-NaCl vs F-CK, F-CK vs Z-CK, and F-NaCl vs Z-NaCl. (c) GO enrichment analysis of Z-NaCl vs Z-CK, and (d) F-NaCl vs F-CK. (e) KEGG enrichment analysis of Z-NaCl vs Z-CK and (f) F-NaCl vs F-CK.

Gene expression profile associated with salinity tolerance

To explore the mechanism behind salt tolerance in *R. rugosa*, we examined DEGs of potential salinity tolerance genes in both the of F-NaCl vs F-CK and Z-NaCl vs Z-CK groups. The functional annotation showed that many DEGs may be related to salt stress and they showed interesting patterns.

In our analysis, we detected 14 DEGs related to ROS production, including eight peroxidase-encoding genes, one peroxygenase-encoding gene, three iron transporter genes, one ferritin gene, and one patatin-like protein-encoding gene. Among them, *POD* (evm.model.Chr6.2566; evm.model.Chr2.1569; evm.model.Chr6.5801; evm.model. Chr3.5028; evm.model.Chr1.2412; evm.model.Chr5.860; evm.model.Chr6.3517) were downregulated. *PXG2* (evm.model.Chr1.280) and *POD4* (evm.model.Chr5.858) were upregulated in NaCl vs CK. Additionally, *PLP2* (evm.model.Chr2.486), with antioxidant activity was upregulated. *Ferritin* (evm.model.Chr4.1192) could maintain the dynamic balance of ROS in plants and its expression was greatly increased after treatment. In contrast, three *VITs* (evm.model.Chr1.4206; evm.model.Chr1.4205; evm.model.Chr6.1138) were correspondingly reduced (Fig. 4).

Soluble sugars can be used as osmotic regulator to maintain osmotic stability when subjected to salt stress. Four *UGTs*

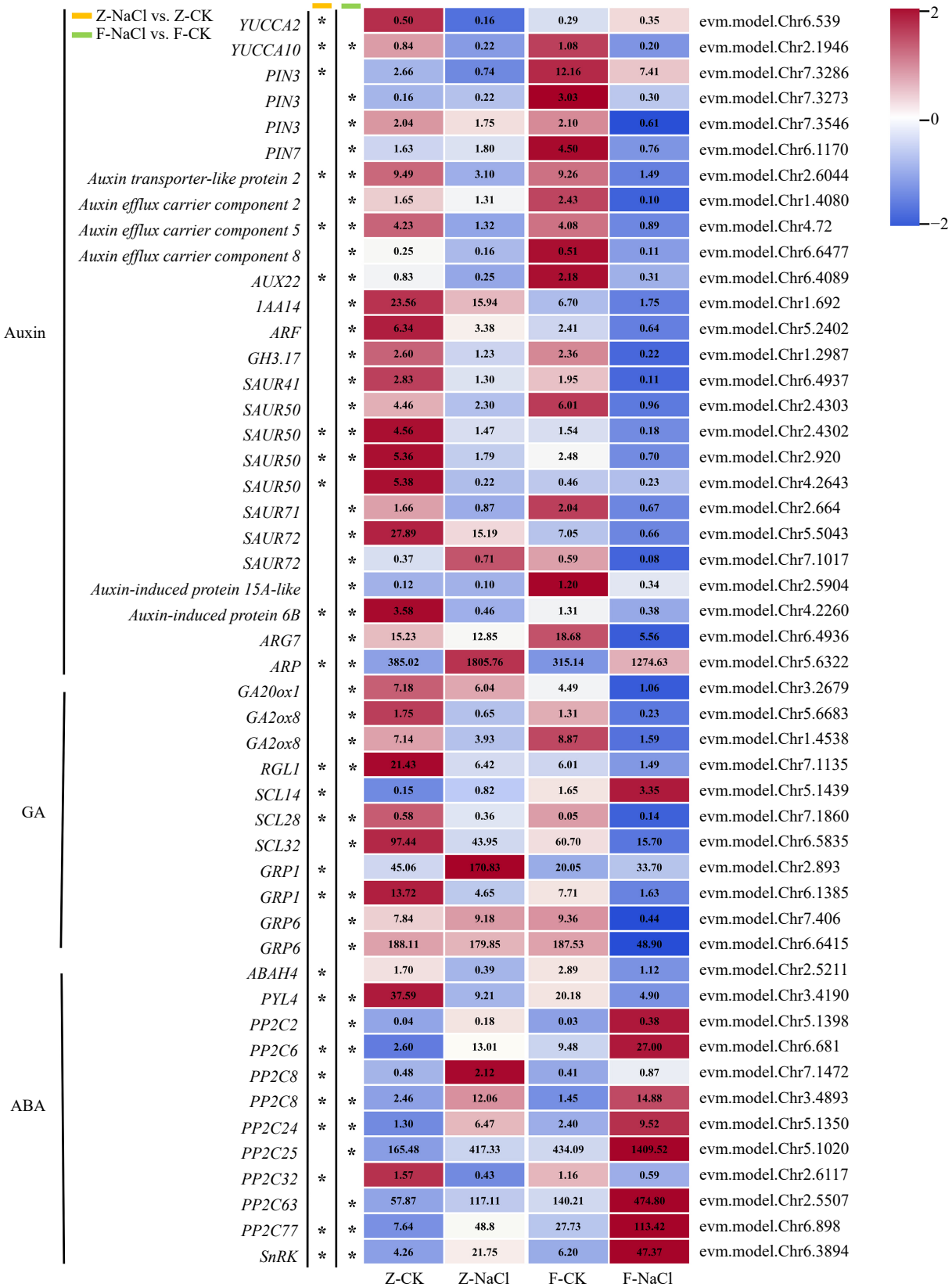

Fig. 3 Heatmap of DEGs associated with phytohormones (* log2| fold changes | ≥ 2, *p*-value < 0.05). ABAH: abscisic acid 8'-hydroxylase; ARF: Auxin response factor; ARG: Auxin-related gene; ARP: auxin-repressed protein; AUX: AUXIN; GA20ox: Gibberellin 20-oxidase; GA2ox: Gibberellin 2-oxidase; GH3: Gretchen Hagen 3; GRP: Gibberellin-regulated protein; IAA: Indole-3-acetic acid; PIN: PIN-formed; PP2C: Protein phosphatase 2C; PYL: Pyrabactin resistance 1-like; RGL1: RGA-like 1; SAUR: Small auxin-up RNA; SCL: Scarcrow-like; SnRK: SNF1-related protein kinase regulatory subunit gamma-like; YUC: YUCCA.

(evm.model.Chr6.5343; evm.model.Chr6.2397; evm.model.Chr7.1386; evm.model.Chr6.5290) exhibited distinct expression patterns, of which three genes (evm.model.Chr6.2397; evm.model.Chr7.1386; evm.model. Chr6.5290) were expressed at higher levels under NaCl treatment. Similarly, *BGL12* (evm.model.Chr5.405), *CESA* (evm.model.Chr1.541), *SWEET* (evm.model.Chr7.1004), PLT6 (evm.model.Chr6.1628), and *AMY2* (evm.model.Chr2.804) were also upregulated. However, the *TPS*-encoding gene (evm.model.Chr7.1386), *EG8/9* (evm.model.Chr1.4280 and evm.model.Chr2.6139), *ERD6* (evm.model.Chr4.510), and BGL8 were downregulated (Fig. 4).

An interesting discovery was that various stress response and resistance protein coding genes had higher expression patterns after salt stress, including *USP* (evm.model.Chr4.2538 and

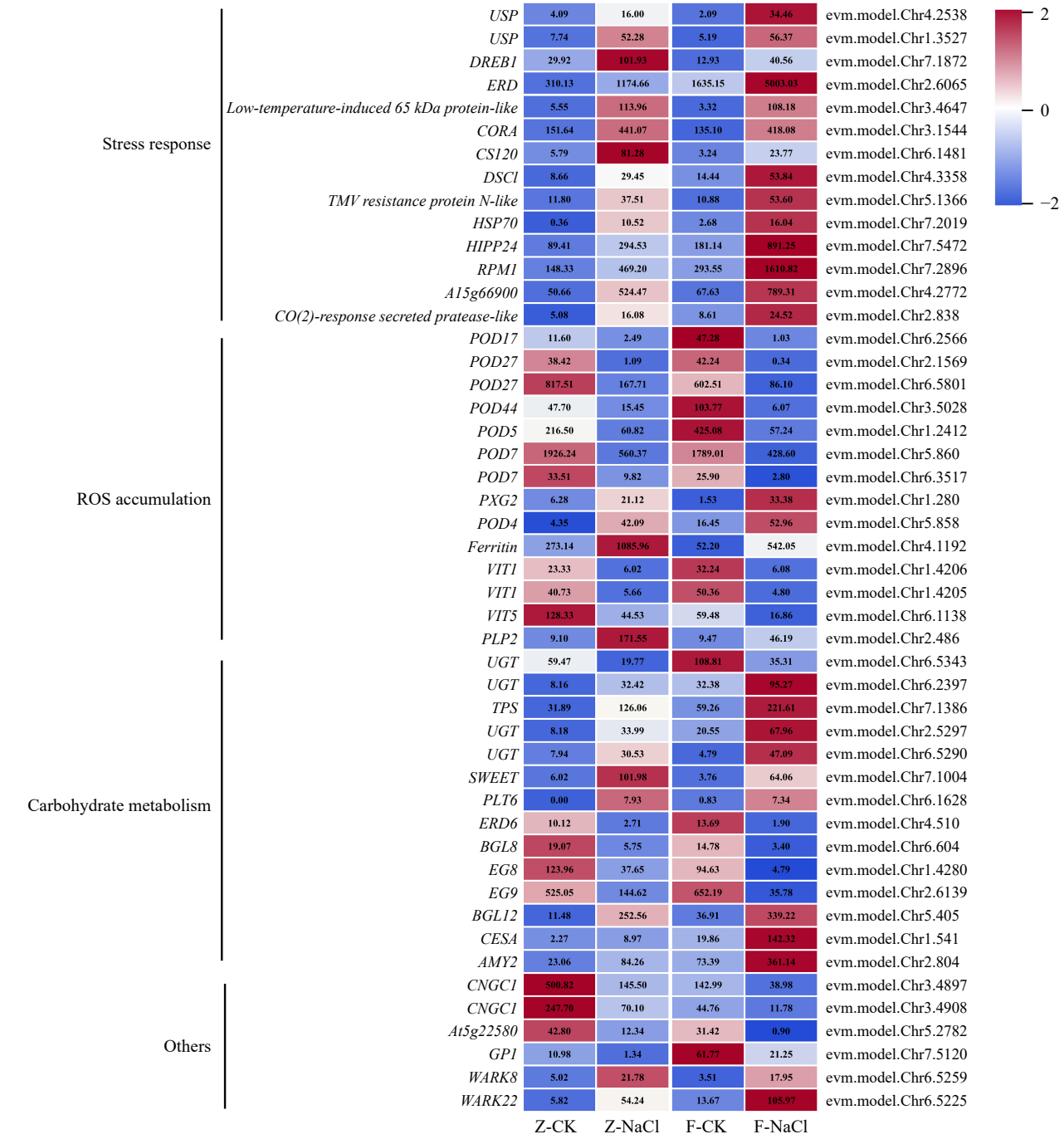

Fig. 4 Expression profile of DEGs associated with salt stress. AMY: Alpha-amylase; BGL: Beta-glucosidase; CESA: Cellulose synthase-like protein; CNGC: Cyclic nucleotide-gated ion channel 1-like; CS: Cold-shock protein; CORA: Cold-regulated protein; DREB: Dehydration-responsive element-binding protein; DSC: Disease resistance-like protein; EG: Endoglucanase; ERD: Early response to dehydration 6-like; ERD: Early-responsive to dehydration; GP1: Vegetative cell wall protein gp1-like; HIPP: Heavy metal-associated isoprenylated plant protein; HSP: Heat shock protein; PLP: Patatin-like protein; PLT: Polyol transporter; POD: Peroxidase; PXG: Peroxygenase; RPM: Resistance to pseudomonas maculicola; SWEET: Sugars will eventually be exported transporter; TPS: Trehalose-6-phosphate synthase; UGT: UDP-glucosyltransferase family protein; USP: universal stress protein; VIT: Vacuolar iron transporter 1-like; WARK: Wall-associated receptor kinase-like.

evm.model.Chr1.3527), *DREB1* (evm.model.Chr7.1872), low-temperature-induced protein (evm.model.Chr3.4647), *CORA* (evm.model.Chr 3.1544), *CS120* (evm.model.Chr6.1481), disease resistance protein (evm.model.Chr4.3358; evm.model.Chr7.2896; evm.model.Chr4.2772), *TMV* resistance protein (evm.model.Chr5.1366), *HSP70* (evm.model.Chr7.2019), *HIPP24* (evm.model.Chr7.5472) and CO(2)-response secreted protease (evm.model.Chr2.838) (Fig. 4). This finding shows that plants exhibit similar responses to different types of stressors.

Additionally, we identified additional genes that could contribute to salt tolerance. Notably, *CNGC1* (evm.model.Chr3.4897 and evm.model.Chr3.4908), one stress-response A/B

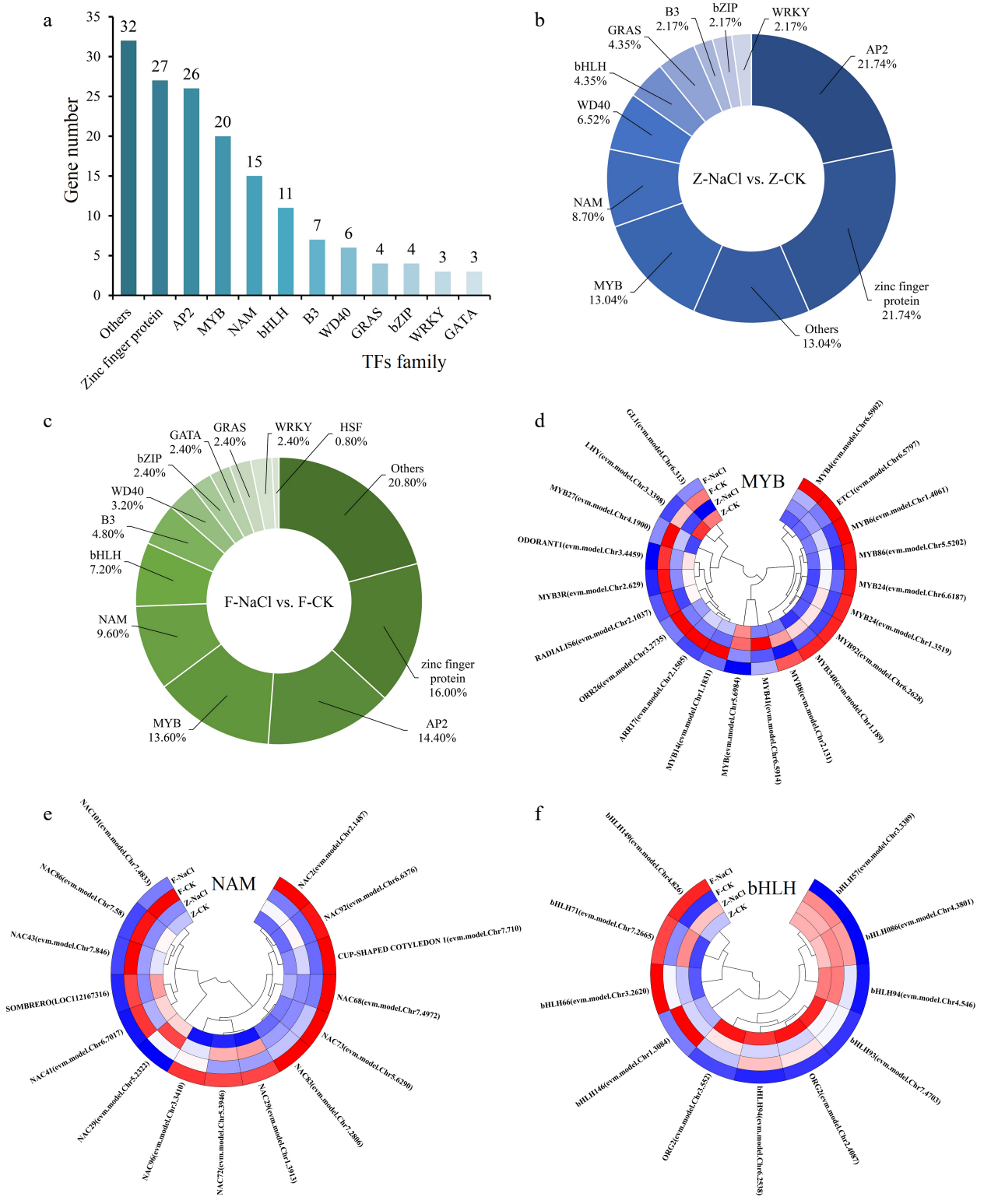

Fig. 5 Transcription factor statistical analysis. (a) Statistics on the number of TFs. (b)–(c) The percentage of TFs in Z-NaCl vs Z-CK, F-NaCl vs F-CK. (d)–(f) Clustering heatmaps of TFs in MYB, NAM, and bHLH.

barrel domain-containing protein At5g22580 (evm.model.Chr 5.2782) and *GP1* (evm.model.Chr7.5120) were downregulated under salt treatment. Equally noteworthy, two *WARK* (evm. model.Chr6.5259 and evm.model.Chr6.5225) was upregulated under salt stress (Fig. 4).

Differential expression analysis of TFs

A total of 158 TFs were identified, and they mainly belonged to the zinc finger protein, AP2, MYB, NAM, bHLH, etc., families (Fig. 5a). Of these TFs, 46 and 125 displayed differential expression in ZZ and FZZ, respectively. In ZZ, TFs mainly belonged to the AP2, MYB, zinc finger protein, NAM, and WD40 families, while in FZZ, they belonged to the AP2, zinc finger protein, MYB, NAM, and bHLH families (Fig. 5b & c). The AP2 family had the largest number of TFs in both ZZ and FZZ. As these families are important in plant stress responses, clustering heatmaps of TFs in MYB, NAM, and bHLH were drawn. Specifically, nine, five, and seven DEGs showed downexpression patterns after salt treatment in MYB, NAM, and bHLH, respectively. Nine, nine, and three DEGs were upregulated in the three families (Fig. 5d–f).

PPI network of DEGs

To predict the potential functions and relationships, the PPI network of DEGs was utilized (Fig. 6). *SCL28* and *E2F1* were core regulators, as they had the most interactions with other genes. *SCL28* interacted with *SCL14*, *SR45a*, and *HSP70* and was further associated with *ERF13* and *ERF4* through *HSP70*. *E2F1* interacted directly with *MYB6*, *GTE3*, *MCM3*, and *MCM2* and was further related to *WRKY45* and *FY*.

qRT-PCR validation of DEGs

We confirmed the RNA-seq results through qRT-PCR. Therefore, we screened 12 DEGs, i.e., auxin-related DEGs (*YUCCA10*, *SAUR50* and *ARP*), ABA-related DEGs (*SnRK*), stress response-related DEGs (*USP* and *HSP70*), DEGs related to ROS accumulation (*POD27* and *VIT1*), DEGs related to sugar metabolism (*UGT* and *TPS*), four TFs (*E2F1*, *SCL28*, *WRKY45*, *MYB92*), and two other DEGs (*CNGC1* and *WARK22*) (Fig. 7). Our findings consistently demonstrated the similarity of expression patterns between qRT-PCR and transcriptome data for these genes.

Discussion

Salt stress causes considerable damage to plant morphology, physiology, and growth. Screening salt-tolerant plant materials can be achieved *via* morphological characteristics, biomass, and physiological indices[18]. By observing the morphology of leaf damage in *R. rugosa* germplasms after salt stress treatment, salt injury was classified into six indices. Two distinct types, namely, salt-tolerant and salt-sensitive, were identified through cluster analysis. Salt stress severely inhibited plant growth, leading to reduced growth indicators. The impact on physiology was reflected in multiple factors, including soluble sugars and proteins, which promote cells to cope with osmotic stresses under salt stress conditions[19]. Salt stress affects plant photosynthesis, which is reflected in the chlorophyll content[20]. Overproduction of ROS induced by salt stress damages plant cells by destroying nucleic acids, lipids, and proteins[21]. ROS synthesis results in the accumulation of MDA, SOD, and POD, which are antioxidant enzymes that play significant defensive roles[22]. Seven physiological indicators were measured in this study, including REC, SS, SP, MDA, SOD, and POD. The physiological indicators significantly increased, except Chl, which showed a decreasing trend. Although the trends of growth

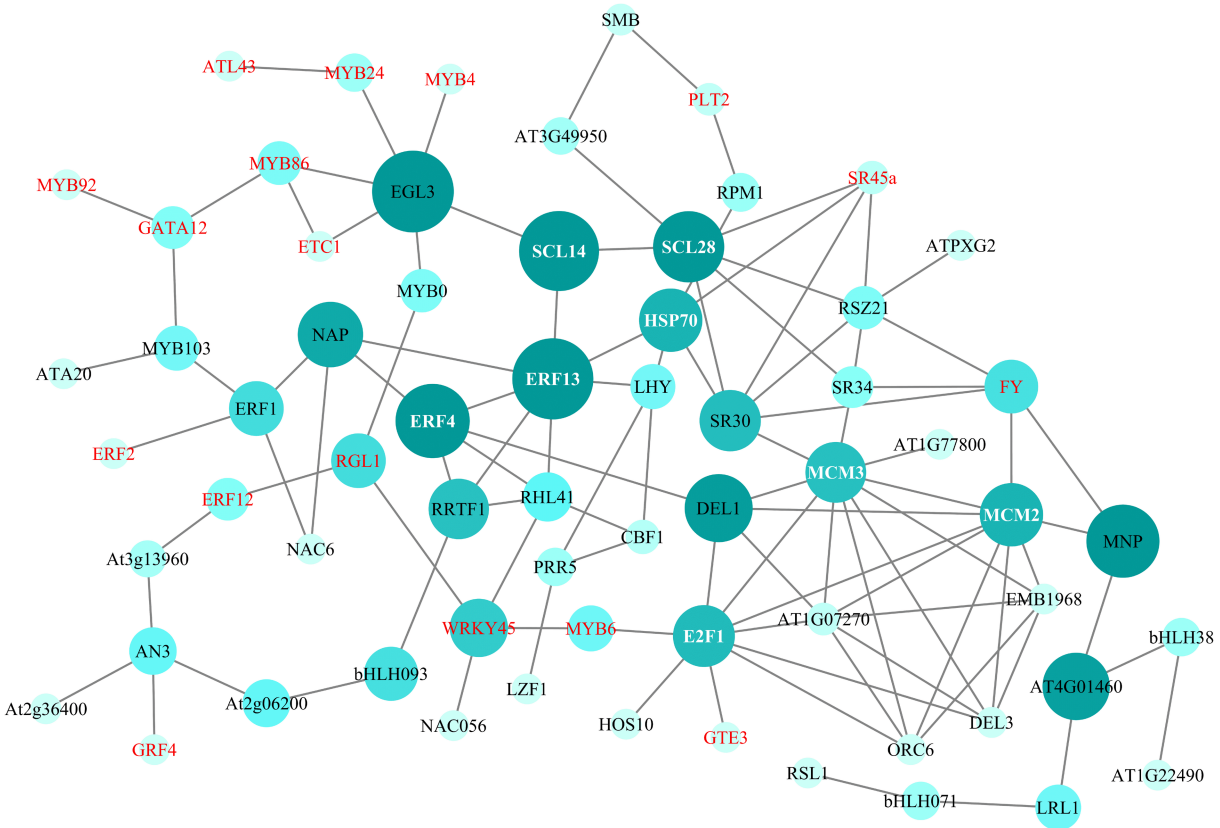

Fig. 6 PPI network of DEGs. Genes in red and white font are DEGs in the transcriptome data of *R. rugosa*.

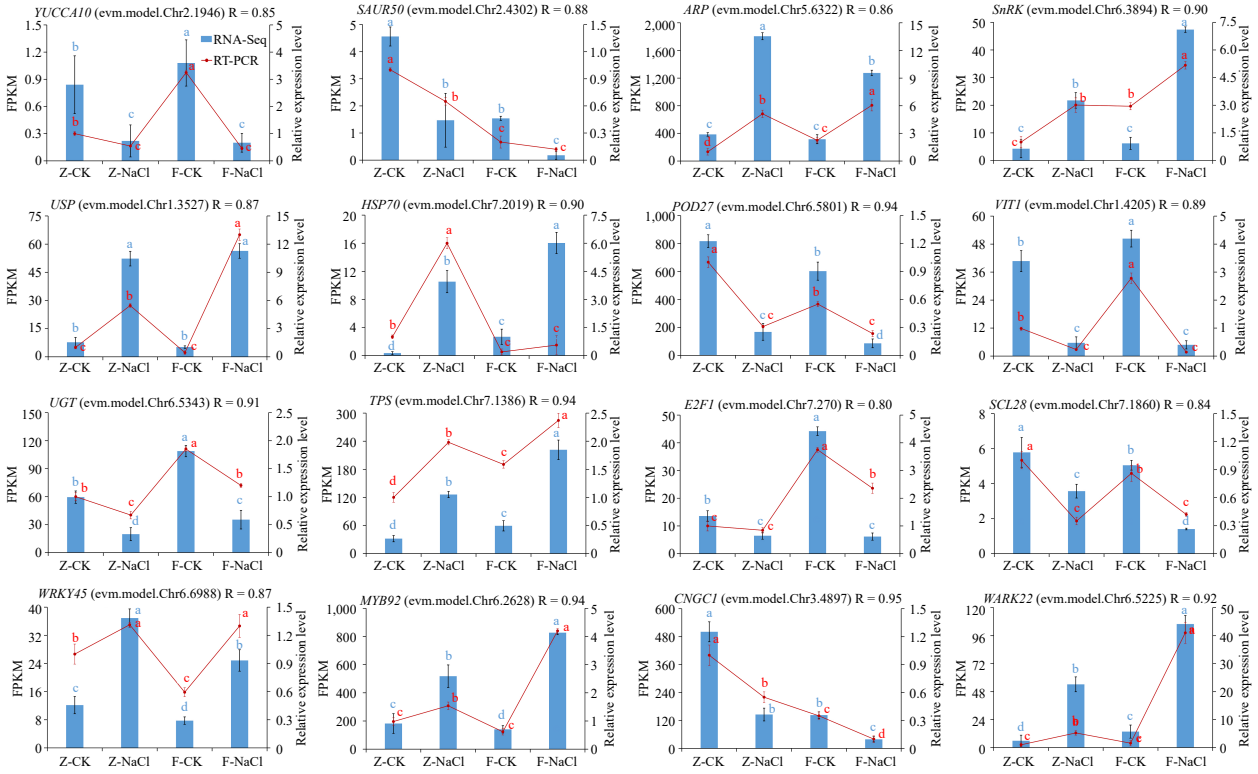

Fig. 7 Quantitative RT-PCR validation of 16 DEGs. Relative expression levels from quantitative RT-PCR and FPKM from the transcriptome of genes are shown on the left and right, respectively. The red line represents the FPKM value in the RNA-seq result. The blue bar represents qRT-PCR results. The different small letter for each expression level indicated significant difference between germplasms at $\alpha = 0.05$.

and physiological changes were consistent across the six germplasms, the degree varied. The variation ranges of ZZ and FZG were evidently smaller or larger than those of other germplasms, indicating stronger salt resistance in ZZ and FZG. Heatmap clustering and principal component analysis confirmed this conclusion. The 16 germplasms were divided into three clusters: salt-tolerant type ('ZZ' and 'FZG'), middle salt-tolerant type ('HC', 'CG', 'HN-2', 'TZ', 'XZ', 'BZZ' and 'TF'), and salt-sensitive type ('NH-1', 'ZZSH', 'ZLYK', 'SXZ', 'TH', 'ZK-2' and 'FZZ').

In this experiment, roots of 'Zizhi' and 'Fenzizhi' at 0 and 4 DAS were collected for transcriptome sequencing. When comparing the salinity stress with the control, the number of downregulated DEGs was more frequent than the number of upregulated DEGs in both cultivars, indicating substantial inhibition of gene expression by salt stress. The comparison between F-NaCl and F-CK revealed a larger number of DEGs compared to Z-NaCl vs Z-CK, particularly the downregulated genes, suggesting a greater impact of NaCl in FZZ than in ZZ.

Phytohormones are essential small chemicals. Relevant research indicates that they play complex and efficient roles under varying environmental conditions[23]. The precise role of IAA metabolism in the response to salt stress is not yet fully understood. Salt stress led to a decrease in both auxin content and the expression level of auxin transporters, given that auxin is a significant growth-promoting hormone[24]. Auxin positive regulators including *YUCCA*, *PIN*, genes coding auxin transporter-like protein and auxin-induced protein, *IAA*, *ARF*, *GH3*, *SAUR*, and auxin-induced protein *ARG7*-like, were downregulated under salt stress in one or both *R. rugosa* cultivars. The YUC family is essential in auxin biosynthesis by regulating the pathway for producing indole-3-pyruvic acid (IPyA)[25]. Overexpression of *YUC* leads to higher capacities for maintaining low ROS levels and confers resistance to salt stress[26]. Auxin influx and efflux are severely impaired under salt stress, subsequently affecting auxin signalling. Salt stress leads to the downregulation of PIN proteins, which are essential for regulating auxin transportation[27]. Auxin signalling pathway proteins Aux/IAA were found to be downregulated due to Nitric Oxide (NO) accumulation caused by salt stress[28]. The interaction between the Aux/IAA proteins and ARFs enables the salt stress response by regulating cis-elements and posttranscriptional processes[27]. The GH3 family of enzymes conjugates IAA with amides. Interestingly, the research found that *GH3* genes are induced under salt stress[29], which was different from our result. Research indicates that the *SAUR* gene positively influences plant root system architecture and enhances abiotic tolerance[30]. Additionally, in the context of salt stress, only one *ARP* gene displayed upregulation. Similarly, an investigation on *Capsicum annuum* revealed the induction of *ARP* in the presence of salt stress[31].

Five genes coding gibberellin-regulated proteins were differentially expressed under salt stress. *GA20ox*, *GA3ox*, and *GA2ox* are essential for the synthesis pathway and inactivation of biologically active GAs[32]. *GA2oxs* can enhance salt tolerance by retarding plant growth[33]. Our research revealed significant downregulation of *GA20ox* and *GA2ox* genes in *R. rugosa*. Reports have indicated that the overexpression of *SCL* can enhance salt tolerance[34]. We identified three *SCL* genes, of which one was induced by salt treatment, and the other two were inhibited. Both RGL and GRP proteins belong to the DELLA family. The overexpression of *RGL3* can mitigate the

inhibitory impact of NO deficiency on salt tolerance[28]. Moreover, the GRP protein is known to be a gibberellin repressor and has been identified as an allergen in fruits[35]. The concentration of GRP protein was influenced by salt stress[36]. According to transcriptome analysis, we found that most *RGL* and *GRP* genes were inhibited under salt stress in *R. rugosa*.

Salt stress induces ABA synthesis, which is the most important stress response hormone. ABAH is an essential enzyme involved in the oxidative degradation of ABA, thus negatively regulating its accumulation[37]. Salt stress was found to suppress the expression of *ABAH4* in *R. rugosa*. Moreover, ABA signalling pathway activation results in an elevation of ABA levels[38]. In the ABA signalling pathway, PYR/PYL/RCARs receptors sense ABA, resulting in the inhibition of *PP2C* activity, which activates *SnRK2*[39]. Our transcriptome analysis showed that there were 11 ABA signalling-related DEGs, including *PYL4*, *SnRK*, and nine *PP2Cs*. The expression profile of *SnRK* in *R. rugosa* under salt stress conditions aligns with previous findings and acts as the most crucial node of ABA signalling[40]. Among the nine *PP2Cs*, only one member showed lower expression under salt treatment, possibly acting as a *SnRK* inhibitor.

Certain proteins exhibit responses to multiple stresses, as many features are shared across these stresses. For instance, *DREB* can be induced by various stressors, including both abiotic and biotic factors[41]. Moreover, pretreatment with salt could prime a plant's response to infection by biotic pathogens[42]. Salinity causes substantial stress by leading to osmotic stress and ionic toxicity, which impacts various biochemical processes and may even result in cell death. In our current research, we found that the expression of multiple stress response protein-coding genes was changed significantly by salt stress in *R. rugosa*, including genes coding *USP*, *DREB1*, *CORA1*, *CS120* and so on. This observation further supports the idea that the response and adaptation mechanisms of plants to various stresses share many common elements.

As previously mentioned, excessive ROS can disrupt the permeability of the plasma membrane and damage DNA and proteins. Plant antioxidant systems consist of various enzymes, such as POD and SOD. Additionally, glutathione-S-transferase (GST) is also included in these systems[43,44]. Fourteen DEGs related to ROS production were identified, with eight *POD* genes being the largest group. Seven of these *POD* genes were downregulated, with a greater reduction in FZZ compared to ZZ. Hence, *POD* may serve as a pivotal regulatory gene in antioxidant system of *R. rugosa*, controlling its response to salt stress. In the present experiment, *PXG2* and *ferritin* were upregulated under salt stress, which is consistent with findings in *Avena chinensis* and *Oryza sativa*[45,46]. This suggests that these two genes may play roles in the salt stress response in *R. rugosa*.

Soluble sugars fulfil a dual role by serving as an energy source for cellular activities and as regulators of intracellular osmotic pressure[47]. Fourteen DEGs (*TPS*, *SWEET*, *PLT6*, and *ERD6*) associated with carbohydrate metabolism and transportation were detected, among which nine genes were upregulated, which was consistent with soluble sugar content. Four *UGT* coding genes exhibited differential expression patterns, and three of them were upregulated under NaCl treatment. Research has demonstrated the positive impact of *UGT* on enhancing plant salt tolerance by promoting flavonoid accumulation[48]. In addition, salt stress has also been shown to activate the expression of *TPS* and sugar transporter genes (*SWEET* and *PLT6*)[49–51]. Sugar metabolism plays an important role in the response to salt stress. Five genes showed downregulation, with the expression levels of *EG8* and *EG9* exhibiting a significant decrease in FZZ compared to ZZ.

The PPI network indicated that the core regulators *SCL28* and *E2F1* had the most interactions with multiple genes. SCL transcription factors are members of the GRAS protein family and are crucial for plant stress resistance. Cruz et al. found the involvement of *SCL28* in stress responses induced by ABA[52]. However, limited findings have been reported regarding their involvement in the plant's salt stress response mechanism. *SCL13* can improve plant growth and increase salt tolerance when overexpressed in both *Arabidopsis thaliana* and *Tamarix hispida*[53,54]. E2F transcription factors interact with MYB-type transcription factors under salt stress conditions to coordinate cell cycles and regulate normal plant growth[55]. Previous findings suggest that these genes may interact to regulate the salt stress response mechanism in *R. rugosa*. However, further verification is necessary to clarify the molecular mechanism underlying these genes.

Author contributions

The authors confirm contribution to the paper as follows: research conception and design: Yu Y, Zhao F; analysis and interpretation of results: Qi S, Wang X, Li X; draft manuscript preparation: Qi S, Wang X; feedback on the analysis and manuscript: Yu Y, Zhao F, Wu Q, Xing S. All authors reviewed the results and approved the final version of the manuscript.

Data availability

The datasets generated during and/or analyzed during the current study are available from the corresponding author on reasonable request.

Acknowledgments

This project was funded by the Shandong Agricultural Seeds Engineering Project (2020LZGC011) and Shandong Provincial Natural Science Foundation (ZR2023MC015).

Conflict of interest

The authors declare that they have no conflict of interest.

Supplementary Information accompanies this paper at (https://www.maxapress.com/article/doi/10.48130/OPR-2023-0021)

Dates

Received 1 August 2023; Accepted 24 November 2023; Published online 15 December 2023

References

1. Ondrasek G, Rengel Z. 2021. Environmental salinization processes: detection, implications & solutions. *Science of the Total Environment* 754:142432

2. Okur B, Örçen N. 2020. Soil salinization and climate change. In *Climate Change and Soil Interactions*, eds. Prasad MNV, Pietrzykowski M. Amsterdam: Elsevier. pp. 331–50. https://doi.org/10.1016/b978-0-12-818032-7.00012-6
3. Hailu B, Mehari H. 2021. Impacts of soil salinity/sodicity on soil-water relations and plant growth in dry land areas: a review. *Journal of Natural Sciences Research* 12:1–10
4. Morton MJL, Awlia M, Al-Tamimi N, Saade S, Pailles Y, et al. 2019. Salt stress under the scalpel – dissecting the genetics of salt tolerance. *The Plant Journal* 97:148–63
5. Eswar D, Karuppusamy R, Chellamuthu S. 2021. Drivers of soil salinity and their correlation with climate change. *Current Opinion in Environmental Sustainability* 50:310–18
6. Syed A, Sarwar G, Shah SH, Muhammad S. 2021. Soil salinity research in 21st century in Pakistan: its impact on availability of plant nutrients, growth and yield of crops. *Communications in Soil Science and Plant Analysis* 52:183–200
7. Ashrafuzzaman M. 2023. Local context of climate change adaptation in the south-western coastal region of Bangladesh. *Sustainability* 15:6664
8. Awlia M, Nigro A, Fajkus J, Schmoeckel SM, Negrão S, et al. 2016. High-throughput non-destructive phenotyping of traits that contribute to salinity tolerance in *Arabidopsis thaliana*. *Frontiers in Plant Science* 7:1414
9. Arif Y, Singh P, Siddiqui H, Bajguz A, Hayat S. 2020. Salinity induced physiological and biochemical changes in plants: an omic approach towards salt stress tolerance. *Plant Physiology and Biochemistry* 156:64–77
10. Liu F, Huang Q, Du Y, Li S, Cai M, et al. 2023. The interference of marine accidental and persistent petroleum hydrocarbons pollution on primary biomass and trace elements sink. *Science of The Total Environment* 883:163812
11. Nowicka B. 2022. Heavy metal–induced stress in eukaryotic algae—mechanisms of heavy metal toxicity and tolerance with particular emphasis on oxidative stress in exposed cells and the role of antioxidant response. *Environmental Science and Pollution Research* 29:16860–911
12. Luo J, Shi W, Li H, Janz D, Luo Z. 2016. The conserved salt-responsive genes in the roots of *Populus* × *canescens* and *Arabidopsis thaliana*. *Environmental and Experimental Botany* 129:48–56
13. Cao W, Liu J, He X, Mu R, Zhou H, et al. 2007. Modulation of ethylene responses affects plant salt-stress responses. *Plant Physiology* 143:707–19
14. Pérez-Patricio M, Camas-Anzueto JL, Sanchez-Alegría A, Aguilar-González A, Gutiérrez-Miceli F, et al. 2018. Optical method for estimating the chlorophyll contents in plant leaves. *Sensors* 18:650
15. Tang Y, Ren J, Liu C, Jiang J, Yang H, et al. 2021. Genetic characteristics and QTL analysis of the soluble sugar content in ripe tomato fruits. *Scientia Horticulturae* 276:109785
16. Yonny ME, Rodríguez Torressi A, Nazareno MA, Cerutti S. 2017. Development of a novel, sensitive, selective, and fast methodology to determine malondialdehyde in leaves of melon plants by ultra-high-performance liquid chromatography-tandem mass spectrometry. *Journal of Analytical Methods in Chemistry* 2017:4327954
17. Ragab G, Saad-Allah K. 2021. Seed priming with greenly synthesized sulfur nanoparticles enhances antioxidative defense machinery and restricts oxidative injury under manganese stress in *Helianthus annuus* (L.) seedlings. *Journal of Plant Growth Regulation* 40:1894–1902
18. Abid M, Zhang Y, Li Z, Bai D, Zhong Y, et al. 2020. Effect of Salt stress on growth, physiological and biochemical characters of Four kiwifruit genotypes. *Scientia Horticulturae* 271:109473
19. Elhakem AH. 2020. Salicylic acid ameliorates salinity tolerance in maize by regulation of phytohormones and osmolytes. *Plant, Soil and Environment* 66:533–41
20. Rahneshan Z, Nasibi F, Moghadam AA. 2018. Effects of salinity stress on some growth, physiological, biochemical parameters and nutrients in two pistachio (*Pistacia vera* L.) rootstocks. *Journal of plant interactions* 13:73–82
21. Kesawat MS, Satheesh N, Kherawat BS, Kumar A, Kim HU, et al. 2023. Regulation of reactive oxygen species during salt stress in plants and their crosstalk with other signaling molecules—current perspectives and future directions. *Plants* 12:864
22. Altaf MA, Hao Y, Shu H, Mumtaz MA, Cheng S, et al. 2023. Melatonin enhanced the heavy metal-stress tolerance of pepper by mitigating the oxidative damage and reducing the heavy metal accumulation. *Journal of Hazardous Materials* 454:131468
23. Zhao B, Liu Q, Wang B, Yuan F. 2021. Roles of phytohormones and their signaling pathways in leaf development and stress responses. *Journal of Agricultural and Food Chemistry* 69:3566–84
24. Yang L, Yang J, Hou C, Shi P, Zhang Y, et al. 2023. Hydrogen sulfide alleviates salt stress through auxin signaling in *Arabidopsis*. *Environmental and Experimental Botany* 211:105354
25. Guo T, Chen K, Dong N, Ye W, Shan J, et al. 2020. *Tillering and small grain 1* dominates the tryptophan aminotransferase family required for local auxin biosynthesis in rice. *Journal of Integrative Plant Biology* 62:581–600
26. Cao X, Yang H, Shang C, Ma S, Liu L, et al. 2019. The roles of auxin biosynthesis YUCCA gene family in plants. *International Journal of Molecular Sciences* 20:6343
27. Ribba T, Garrido-Vargas F, O'Brien JA. 2020. Auxin-mediated responses under salt stress: from developmental regulation to biotechnological applications. *Journal of Experimental Botany* 71:3843–53
28. Shi H, Liu W, Wei Y, Ye T. 2017. Integration of auxin/indole-3-acetic acid 17 and RGA-LIKE3 confers salt stress resistance through stabilization by nitric oxide in *Arabidopsis*. *Journal of Experimental Botany* 68:1239–49
29. Kirungu JN, Magwanga RO, Lu P, Cai X, Zhou Z, et al. 2019. Functional characterization of *Gh_A08G1120* (*GH3.5*) gene reveal their significant role in enhancing drought and salt stress tolerance in cotton. *BMC Genetics* 20:62
30. Guo Y, Jiang Q, Hu Z, Sun X, Fan S, et al. 2018. Function of the auxin-responsive gene *TaSAUR75* under salt and drought stress. *The Crop Journal* 6:181–90
31. Lee J, Han CT, Hur Y. 2013. Molecular characterization of the *Brassica rapa* auxin-repressed, superfamily genes, *BrARP1* and *BrDRM1*. *Molecular Biology Reports* 40:197–209
32. Yoshida H, Takehara S, Mori M, Ordonio RL, Matsuoka M. 2020. Evolution of GA metabolic enzymes in land plants. *Plant and Cell Physiology* 61:1919–34
33. Uçarlı C. 2021. Physiological and molecular effects of exogenous gibberellin (GA3) treatment on germination of barley seeds under salt stress. *Adıyaman University Journal of Science* 11:227–43
34. Ma H, Liang D, Shuai P, Xia X, Yin W. 2010. The salt- and drought-inducible poplar GRAS protein SCL7 confers salt and drought tolerance in *Arabidopsis thaliana*. *Journal of Experimental Botany* 61:4011–19
35. Inomata N, Miyakawa M, Ikeda N, Oda K, Aihara M. 2018. Identification of gibberellin-regulated protein as a new allergen in orange allergy. *Clinical & Experimental Allergy* 48:1509–1520
36. Muhammad I, Li W, Jing X, Zhou M, Shalmani A, et al. 2019. A systematic *in silico* prediction of gibberellic acid stimulated GASA family members: a novel small peptide contributes to floral architecture and transcriptomic changes induced by external stimuli in rice. *Journal of Plant Physiology* 234–235:117–32
37. Gu N, Zhang X, Gu X, Zhao L, Godana EA, et al. 2021. Transcriptomic and proteomic analysis of the mechanisms involved in enhanced disease resistance of strawberries induced by *Rhodotorula mucilaginosa* cultured with chitosan. *Postharvest Biology and Technology* 172:111355

38. Wang N, Wang X, Zhang H, Liu X, Shi J, et al. 2021. Early ABA-stimulated maintenance of Cl^- homeostasis by mepiquat chloride priming confers salt tolerance in cotton seeds. *The Crop Journal* 9:387–99
39. Lin Z, Li Y, Wang Y, Liu X, Ma L, et al. 2021. Initiation and amplification of *SnRK2* activation in abscisic acid signaling. *Nature Communications* 12:2456
40. Ye Y, Jia X, Xue M, Gao Y, Yue H, et al. 2022. *MpSnRK2.10* confers salt stress tolerance in apple via the ABA signaling pathway. *Scientia Horticulturae* 298:110998
41. Akbudak MA, Filiz E, Kontbay K. 2018. *DREB2* (dehydration-responsive element-binding protein 2) type transcription factor in sorghum (*Sorghum bicolor*): genome-wide identification, characterization and expression profiles under cadmium and salt stresses. *3 Biotech* 8:426
42. Yang Y, Yin J, Huang L, Li J, Chen D, et al. 2019. Salt enhances disease resistance and suppresses cell death in ceramide kinase mutants. *Plant Physiology* 181:319–31
43. Noctor G, Mhamdi A, Foyer CH. 2014. The roles of reactive oxygen metabolism in drought: not so cut and dried. *Plant Physiology* 164:1636–48
44. Arnao MB, Hernández-Ruiz J. 2019. Melatonin: a new plant hormone and/or a plant master regulator? *Trends in Plant Science* 24:38–48
45. Gao W, Feng Z, Bai Q, He J, Wang Y. 2019. Melatonin-mediated regulation of growth and antioxidant capacity in salt-tolerant naked oat under salt stress. *International Journal of Molecular Sciences* 20:1176
46. Du Q, Campbell M, Yu H, Liu K, Walia H, et al. 2019. Network-based feature selection reveals substructures of gene modules responding to salt stress in rice. *Plant Direct* 3:e00154
47. Saddhe AA, Manuka R, Penna S. 2021. Plant sugars: homeostasis and transport under abiotic stress in plants. *Physiologia Plantarum* 171:739–55
48. Li Q, Yu H, Meng X, Lin J, Li Y, et al. 2018. Ectopic expression of glycosyltransferase UGT76E11 increases flavonoid accumulation and enhances abiotic stress tolerance in *Arabidopsis*. *Plant Biology* 20:10–19
49. Chan Z, Grumet R, Loescher W. 2011. Global gene expression analysis of transgenic, mannitol-producing, and salt-tolerant *Arabidopsis thaliana* indicates widespread changes in abiotic and biotic stress-related genes. *Journal of Experimental Botany* 171:4787–803
50. Mathan J, Singh A, Ranjan A. 2021. Sucrose transport in response to drought and salt stress involves ABA-mediated induction of *OsSWEET13* and *OsSWEET15* in rice. *Physiologia Plantarum* 171:620–37
51. Sarkar AK, Sadhukhan S. 2022. Imperative role of trehalose metabolism and trehalose-6-phosphate signaling on salt stress responses in plants. *Physiologia Plantarum* 174:e13647
52. Cruz TMD, Carvalho RF, Richardson DN, Duque P. 2014. Abscisic acid (ABA) regulation of *Arabidopsis* SR protein gene expression. *International Journal of Molecular Siences* 15:17541–64
53. Zhang S, Li X, Fan S, Zhou L, Wang Y. 2020. Overexpression of *HcSCL13*, a *Halostachys caspica* GRAS transcription factor, enhances plant growth and salt stress tolerance in transgenic *Arabidopsis*. *Plant Physiology and Biochemistry* 151:243–54
54. Lei X, Fang J, Lv J, Li Z, Liu Z, et al. 2023. Overexpression of *ThSCL32* confers salt stress tolerance by enhancing *ThPHD3* gene expression in *Tamarix hispida*. *Tree Physiology* 43:1444–53
55. Okumura T, Nomoto Y, Kobayashi K, Suzuki T, Takatsuka H, et al. 2021. MYB3R-mediated active repression of cell cycle and growth under salt stress in *Arabidopsis thaliana*. *Journal of Plant Research* 134:261–77